2011

Connections of the superior paraolivary nucleus of the rat: II. Reciprocal connections with the tectal longitudinal column

Antonio Vinuela
University of Salamanca

M-Auxiliadora Aparicio
University of Salamanca

Albert S. Berrebi
West Virginia University

Enrique Saldana
University of Salamanca

frontiers in
NEUROANATOMY

ORIGINAL RESEARCH ARTICLE
published: 22 February 2011
doi: 10.3389/fnana.2011.00001

Connections of the superior paraolivary nucleus of the rat: II. Reciprocal connections with the tectal longitudinal column

Antonio Viñuela[1,2], M.-Auxiliadora Aparicio[1,3], Albert S. Berrebi[4] and Enrique Saldaña[1,2]*

[1] *Laboratory for the Neurobiology of Hearing, Neuroscience Institute of Castilla y León, University of Salamanca, Salamanca, Spain*
[2] *Department of Cell Biology and Pathology, Medical School, University of Salamanca, Salamanca, Spain*
[3] *Department of Pathology, Clinical University Hospital of Salamanca, Salamanca, Spain*
[4] *Department of Otolaryngology, The Sensory Neuroscience Research Center, West Virginia University School of Medicine, Morgantown, WV, USA*

Edited by:
Enrico Mugnaini, Northwestern University, USA

Reviewed by:
Marina Bentivoglio, University of Verona, Italy
Douglas L. Oliver, University of Connecticut Health Center, USA
Donata Oertel, University of Wisconsin, USA
Joe Adams, Massachusetts Eye and Ear Infirmary, USA

***Correspondence:**
Enrique Saldaña, Laboratory for the Neurobiology of Hearing, Neuroscience Institute of Castilla y León, University of Salamanca, Salamanca 37007, Spain.
e-mail: saldana@usal.es

The superior paraolivary nucleus (SPON), a prominent GABAergic center of the mammalian auditory brainstem, projects to the ipsilateral inferior colliculus (IC) and sends axons through the commissure of the IC (CoIC). Herein we demonstrate that the SPON is reciprocally connected with the recently discovered tectal longitudinal column (TLC). The TLC is a long and narrow structure that spans nearly the entire midbrain tectum longitudinally, immediately above the periaqueductal gray matter (PAG) and very close to the midline. Unilateral injections of biotinylated dextran into the SPON of the rat label abundant terminal fibers in the TLC of both sides, with an ipsilateral predominance. The SPON provides a dense innervation of the entire rostrocaudal extent of the ipsilateral TLC, and a relatively sparser innervation of the caudal and rostral portions of the contralateral TLC. SPON fibers reach the TLC by two routes: as collaterals of axons of the CoIC, and as axons that circumvent the ipsilateral IC before traveling in the deep layers of the superior colliculus (SC). The density of these projections identifies SPON as a significant source of input to the TLC. Other targets of the SPON discovered in this study include the deep layers of the SC and the PAG. The same experiments reveal numerous labeled cell bodies in the TLC, interspersed among the labeled SPON fibers. This observation suggests that the SPON is a significant target of TLC projections. The discovery of novel reciprocal connections between the SPON and the TLC opens unexpected avenues for investigation of sound processing in mammalian brainstem circuits.

Keywords: auditory brainstem, commissure of the inferior colliculus, superior colliculus, periaqueductal gray matter, superior olivary complex, biotinylated dextran amine, tract-tracing

INTRODUCTION

The tectal longitudinal column (TLC) spans the midbrain tectum longitudinally, immediately above the periaqueductal gray matter (PAG) and very close to the midline. In the rat, the TLC extends approximately 3.5 mm, from the caudal end of the commissure of the inferior colliculus (CoIC) to the rostral end of the commissure of the superior colliculus (CoSC), and occupies what has traditionally been considered the medial-most region of the deep superior colliculus (SC) and the medial-most region of the inferior colliculus (IC). Despite measuring only 250–350 μm in diameter, more than 11,500 neurons are packed within this long and narrow structure (Saldaña et al., 2007).

The caudal and rostral thirds of the TLC are crossed by the CoIC and by the CoSC (Saldaña et al., 2007), respectively, suggesting that these fiber tracts are a preferred pathway of entry for afferent inputs to the TLC. The CoIC contains mostly commissural axons of the IC, as well as axons from other sources or destined for other targets (reviewed by Saldaña and Merchán, 2005). These include axons from various subcollicular auditory nuclei, namely the sagulum and nuclei of the lateral lemniscus (González-Hernández et al., 1987; Henkel and Shneiderman 1988; Hutson et al., 1991; Bajo et al., 1993). Recently, it has been demonstrated that the superior paraolivary nucleus (SPON), a prominent cell group of the superior olivary complex (SOC), also projects axons across the CoIC (Saldaña et al., 2009). Thus, we set forth to investigate whether the SPON, which is likely the caudal-most auditory center sending projections across the CoIC, innervates the TLC. We chose to carry out this investigation in rats because the TLC has been best characterized in this species (Saldaña et al., 2007; Marshall et al., 2008; Aparicio et al., 2010); moreover, abundant information is available concerning the structure, connections and physiology of the rat SPON (Kulesza Jr. and Berrebi, 2000; Saldaña and Berrebi, 2000; Kulesza Jr. et al., 2003, 2007; Kadner et al., 2006; Kadner and Berrebi, 2008; Saldaña et al., 2009).

MATERIALS AND METHODS

Thirteen female albino rats (body weight 190–210 g) with clean ear canals and no sign of middle ear infection were used in this study. These specimens were also used for the study of SPON projections to the IC described in a previous article (Saldaña et al., 2009). All animals were cared for and used in compliance with European Union regulations concerning the use of animals in biomedical research, and the experimental procedures were approved and supervised by the Animal Care and Use Committee of the University of Salamanca.

For surgical procedures, including the transcardial perfusion of fixatives, all animals were deeply anesthetized with a mixture of ketamine HCl (80 mg/kg body weight) and xylazine (6 mg/kg body weight) administered intramuscularly. Animal suffering was minimized by monitoring the depth of anesthesia often, carefully attending to physiological cues such as rate and depth of respiration and reflex activity. Supplemental doses of anesthetics were given as needed to maintain deep anesthesia throughout all procedures.

Glass micropipettes loaded with the neuroanatomical tracer biotinylated dextran amine (BDA, 10,000 MW, Molecular Probes, Eugene, OR, USA; 10% in 0.1 M sodium phosphate buffer, pH 7.4) were lowered into the SPON of deeply anesthetized rats using stereotaxic coordinates (Paxinos and Watson, 2007). To avoid damage to the prominent transverse sinus, the pipettes were lowered into the brain *via* a dorsocaudal to ventrorostral approach, so that their trajectory formed a 16° angle with the coronal plane. The tracer was delivered by iontophoresis using a pulsed 5 μA DC positive current (7 s on/7 s off) for 5–15 min. The current was then stopped and the pipette left in place for an additional 15–20 min prior to withdrawal in order to minimize leakage of the tracer along the injection tract.

Following 7–10 days survival, the rats were anesthetized deeply and their brains fixed by transcardial perfusion of buffered 4% formaldehyde (prepared from freshly depolymerized paraformaldehyde) and 0.1% glutaraldehyde. After cryoprotection in 30% sucrose in phosphate buffer, the brains were cut coronally on a freezing microtome at a thickness of 40 μm. To visualize the tracer, the sections were first processed by the avidin–biotin–peroxidase complex procedure following the manufacturer's specifications (ABC, Vectastain, Vector Labs, Burlingame, CA, USA), and then by standard histochemistry for peroxidase, with or without heavy-metal intensification (Vetter et al., 1993). For cytoarchitectural reference, every fourth section was counterstained with cresyl violet.

Sections were photographed at high resolution using a Zeiss Axioskop 40 microscope equipped with a Zeiss AxioCam MRc 5 digital camera and 2.5× (NA 0.075), 5× (NA 0.15), 10× (NA 0.30), 20× (NA 0.50), and 40× (NA 0.75) plan semi-apochromatic objective lenses. Image brightness and contrast were adjusted with Adobe Photoshop software (Adobe Systems Incorporated, San Jose, CA, USA), and the illustrations were arranged into plates using Canvas software (ACD Systems of America, Inc., Miami, FL, USA).

To generate the drawings of **Figure 2**, the sections were first photographed at high resolution with the 5× objective lens. At this magnification, several micrographs were needed to photograph every section. These photographs were then arranged and fitted using Adobe Photoshop software to create a large mosaic image of the section. The resulting digital image was imported into Canvas software. To increase the resolution of the final image, a new layer was created over the digital image and each labeled fiber contained within the original micrograph was redrawn digitally using Canvas' freehand drawing tool. This digital procedure allowed us to subsequently adjust the thickness of the lines. The new digital layer, without the underlying micrograph, was finally saved as a TIFF file.

A similar procedure was used to produce the plots showing the distribution of presumed labeled synaptic boutons in **Figures 6 and 7**. To convey a clear impression of synaptic bouton density, each plot of **Figure 7** was subsequently transferred to a Photoshop document and blurred using a Gaussian filter with a 20-pixel square matrix.

RESULTS

The present results are based on 13 cases with single injections of BDA into the SPON. In 12 cases, the injection sites were localized within the SPON, without encroaching upon neighboring structures (e.g., **Figure 1A**). In the other case (case 99014), the injection site encroached upon the medial superior olive. The mediolateral diameter of the center of the injection sites ranged from 150 to 380 μm. **Figure 1B** shows schematically the injection site of seven representative cases.

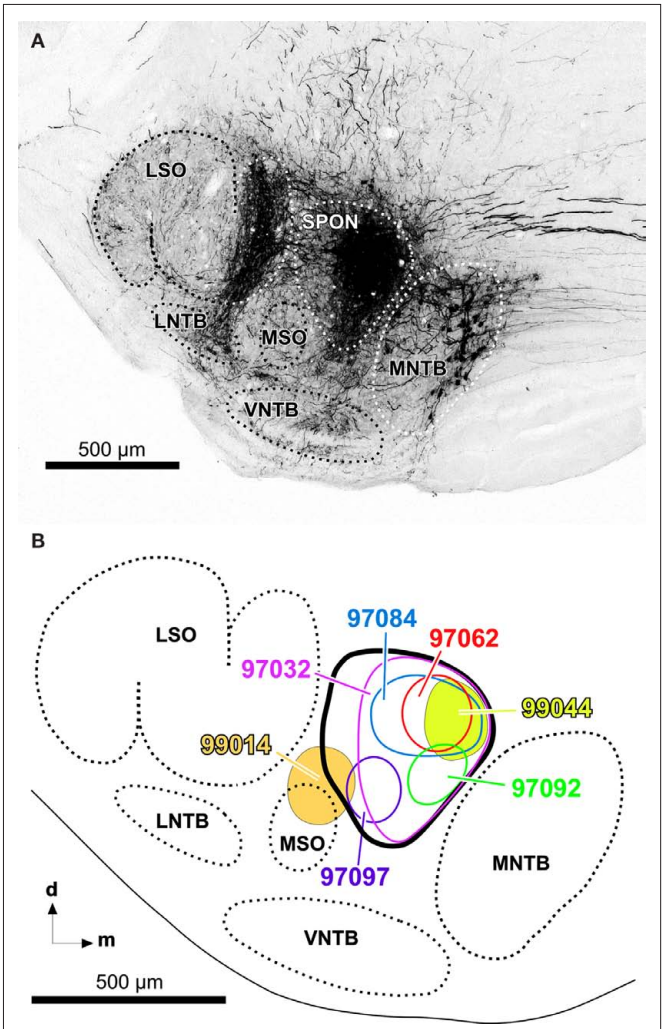

FIGURE 1 | (A) Representative injection site of BDA into the SPON of the rat. Digital photomicrograph of a coronal section through the central rostrocaudal third of the left superior olivary complex from a case whose injection site is wholly contained within the limits of the SPON (case 97062). Retrogradely labeled neuronal cell bodies in the medial nucleus of the trapezoid body (MNTB) and their fibers and terminals in the lateral superior olive (LSO) are evident. For more information on the interpretation of the neurons and fibers labeled following injections of BDA into the SPON, see Saldaña et al. (2009). **(B)** Schematic representation of the sizes and locations of the injection sites of various representative cases. Other abbreviations: d, dorsal; LNTB, lateral nucleus of the trapezoid body; m, medial; MSO, medial superior olive; VNTB, ventral nucleus of the trapezoid body.

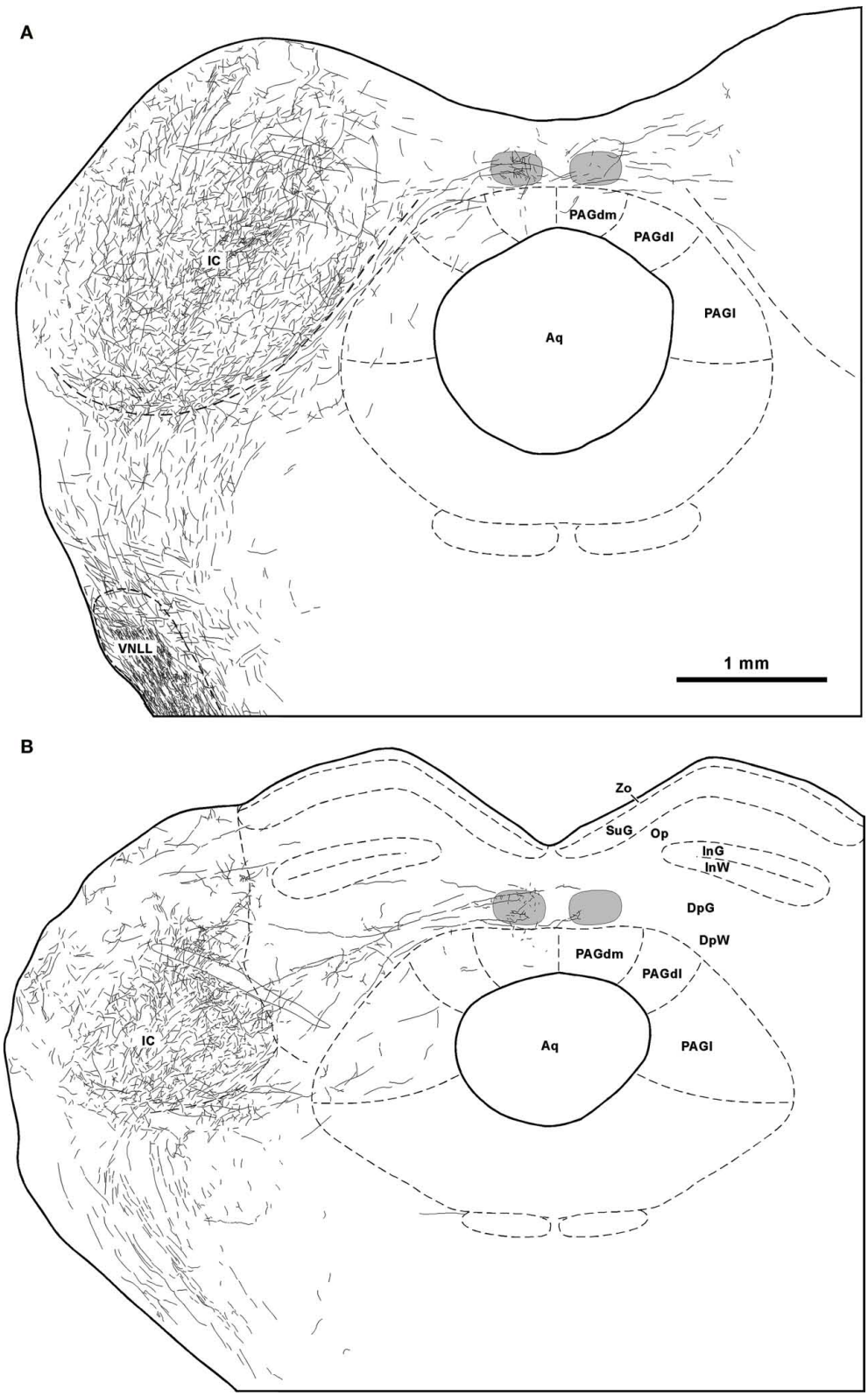

FIGURE 2 | ***(Continued)***

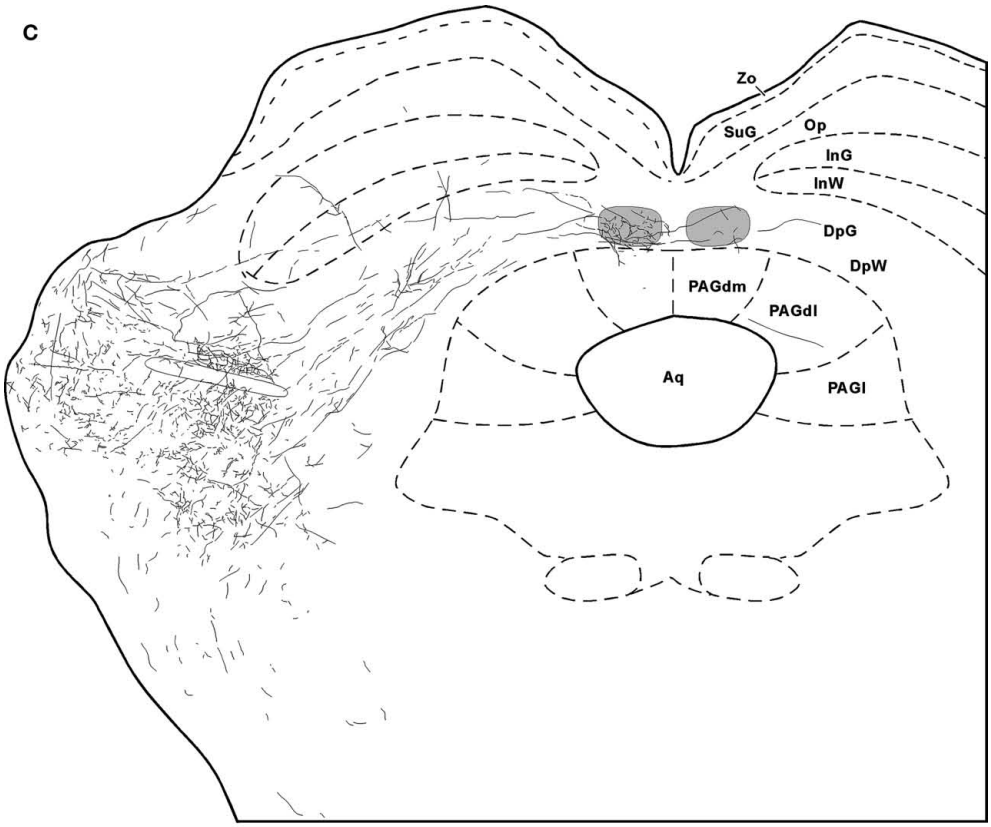

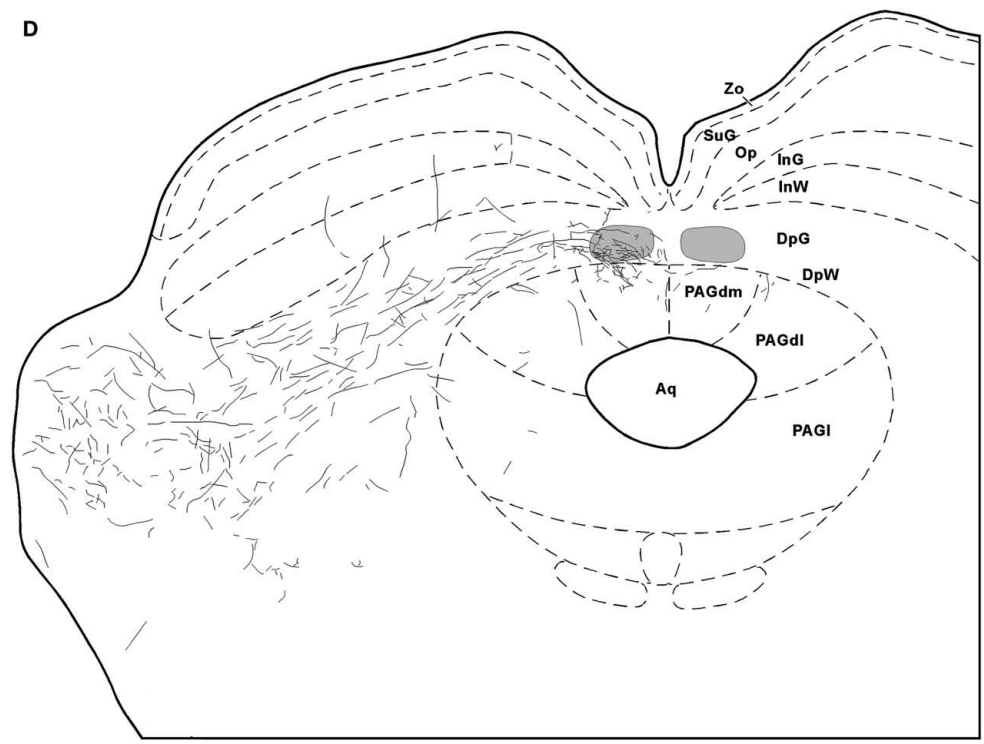

FIGURE 2 | ***(Continued)***

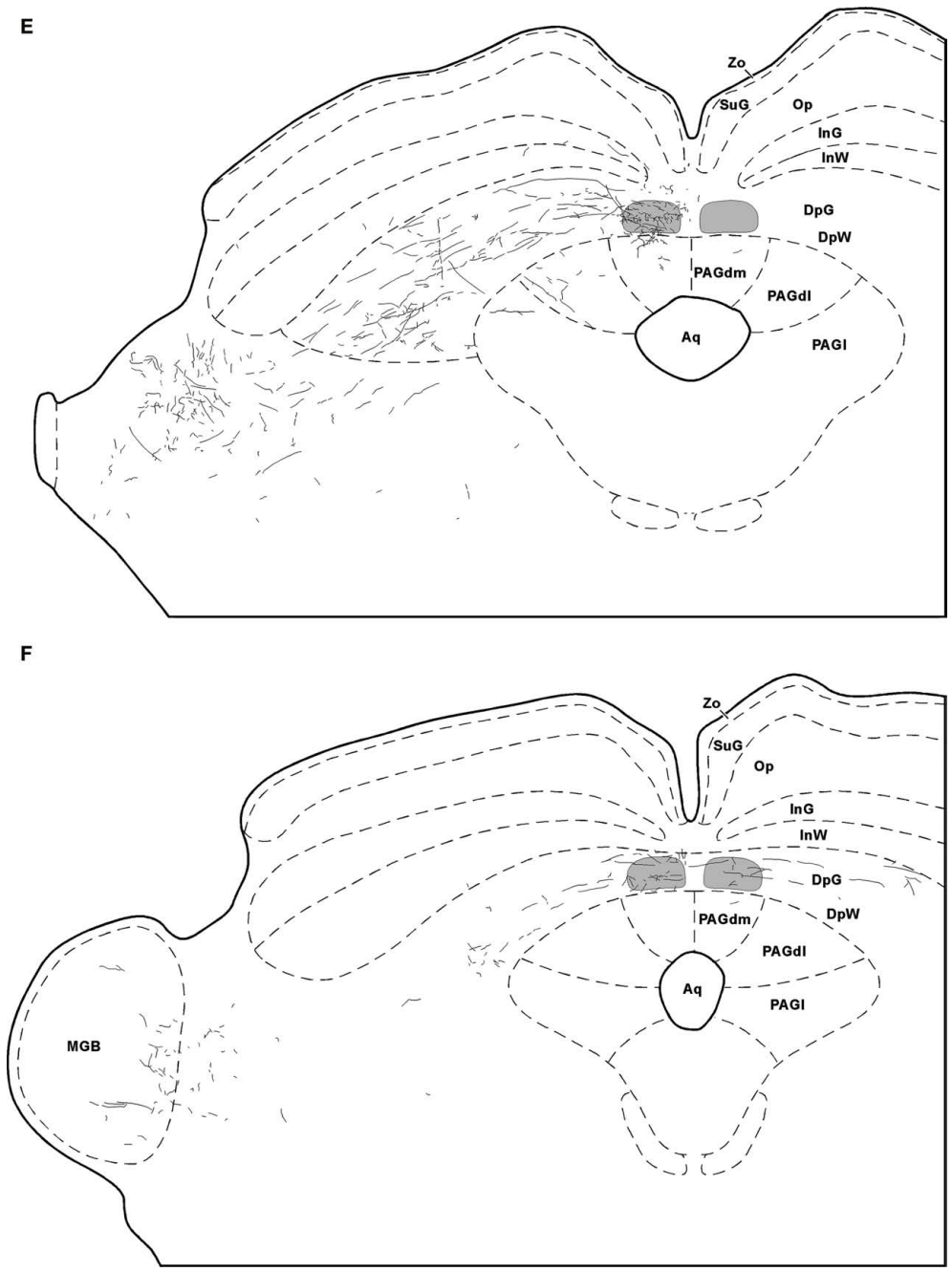

FIGURE 2 | Trajectory and distribution of SPON axons. (A–F) Drawings of coronal sections of the midbrain illustrating axons labeled following a single injection of BDA into the left SPON. Case 97084, whose injection site is depicted in **Figure 1B**. The sections have been ordered from caudal to rostral and illustrate levels similar to those shown in **Figure 3**. The TLC is represented in light gray and the scale bar in **(A)** applies to all six drawings. Abbreviations of SC layers: DpG, deep gray; DpW, deep white; InG, intermediate gray; InW, intermediate white; Op, stratum opticum; SuG, superficial gray; Zo, stratum zonale. Abbreviations of periaqueductal gray matter (PAG) columns: PAGl, lateral column; PAGdl, dorsolateral column; PAGdm, dorsomedial column. Other abbreviations: Aq, cerebral aqueduct; IC, inferior colliculus; MGB, medial geniculate body; VNLL, ventral nucleus of the lateral lemniscus.

PROJECTION FROM THE SPON TO THE TLC

Labeled SPON axons, easily recognizable by their large caliber (>1.2 μm), exit the injection site and travel rostrally, dorsally, and laterally to join the medial-most aspect of the ipsilateral lateral lemniscus, through which they ascend toward the midbrain tectum without entering the nuclei of the lateral lemniscus. Most SPON axons then penetrate into the IC, where they create dense terminal fields in all IC subdivisions. Some SPON axons that reach the dorsal cortex

of the IC extend dorsomedially and cross the CoIC, to innervate the dorsal cortex of the contralateral IC. The distribution of labeled fibers in the nuclei of the lateral lemniscus and the IC following injections of BDA into the SPON has been described previously (Saldaña et al., 2009) and will therefore not be considered further in this account.

Those SPON axons destined to innervate the TLC do so by two different routes. The first route is taken by some of the axons traveling in the CoIC (**Figures 2A,B, 3A,B, and 4A**). These fibers give off one or more collaterals within the ipsilateral TLC and/or, less frequently, within the contralateral TLC. Occasionally individual labeled SPON fibers give off collaterals to both the ipsilateral and contralateral TLCs (**Figure 4A**). All of these collaterals are usually thin and tend to run either vertically within the CoIC or rostrally, so that the latter course caudorostrally within the TLC.

The second, more prominent pathway of entry into the TLC is formed by SPON axons that circumvent the ipsilateral IC ventromedially or ventrorostrally to reach the SC. These fibers then run dorsomedially through the deep layers of the SC to reach the

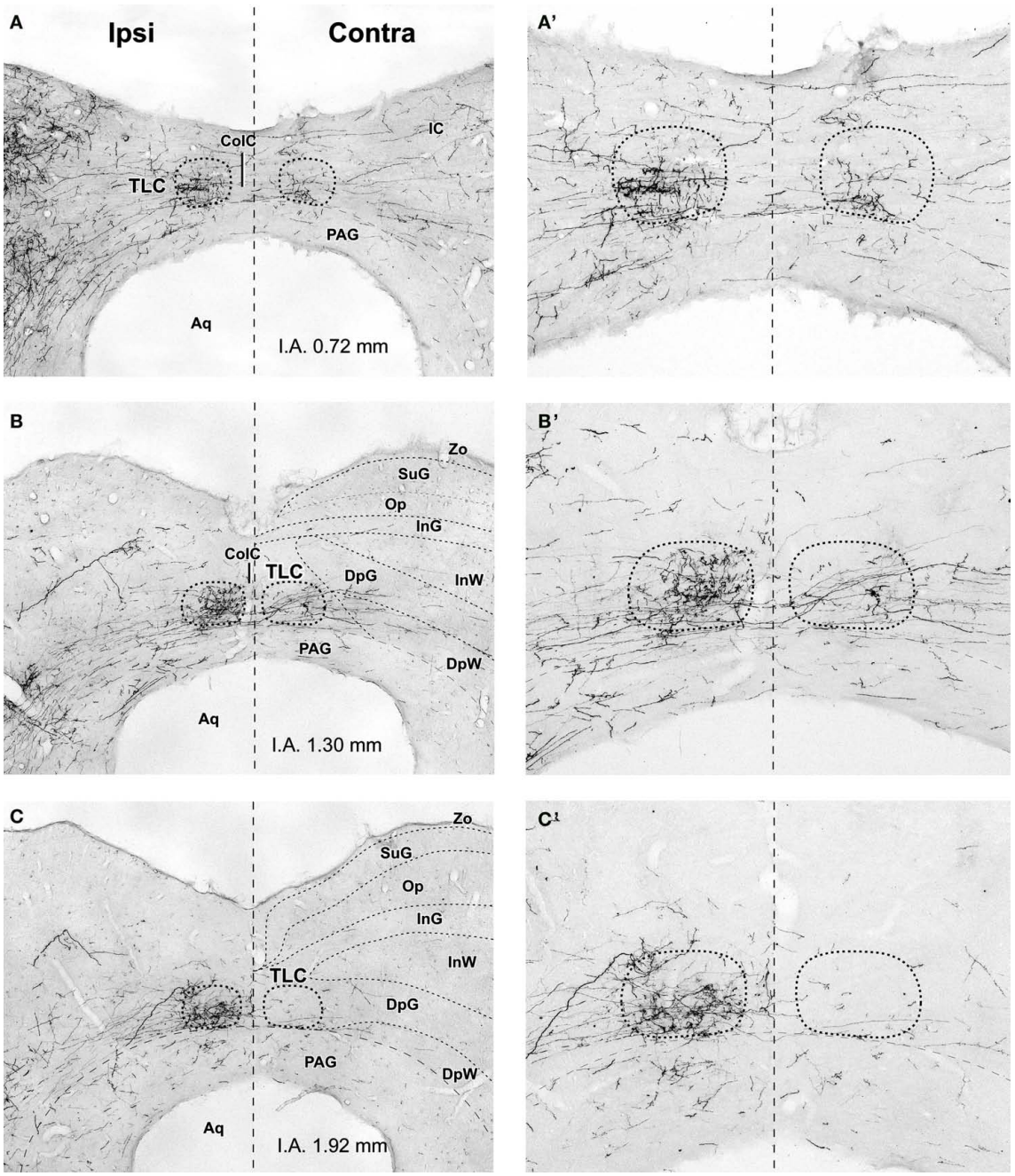

FIGURE 3 | ***(Continued)***

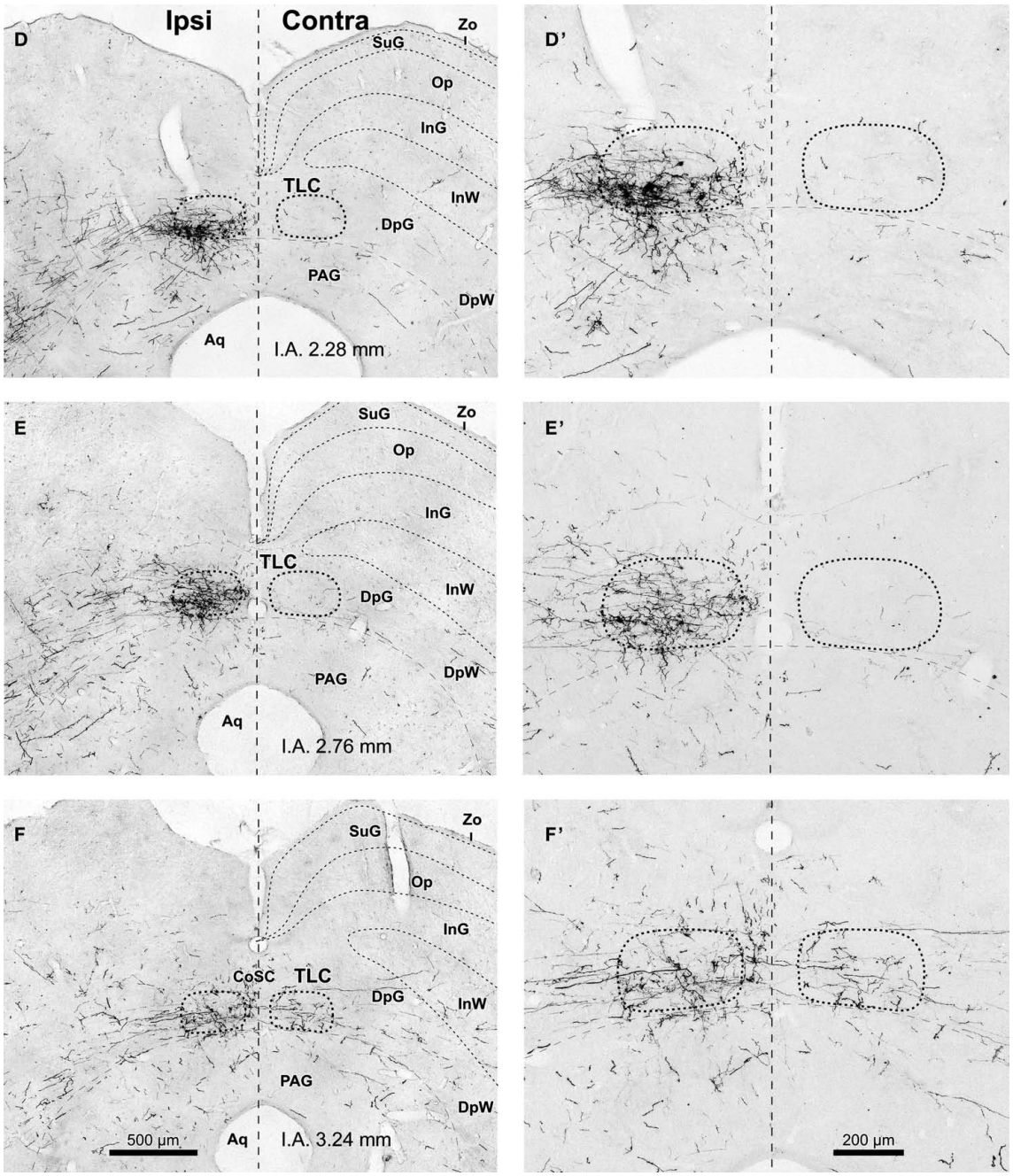

FIGURE 3 | Labeled SPON axons in the TLC. (A–F, A′–F′) Digital micrographs of six coronal sections taken from different rostrocaudal levels of the midbrain tectum of case 97084, whose injection site is depicted in **Figure 1B**. Sections have been ordered from caudal to rostral. The number at the bottom of each panel indicates the distance in millimeters between the depicted plane and the interaural coronal plane (I.A.). Micrographs in the right column show higher magnification views of the corresponding micrograph in the left column. Vertical dashed lines indicate the midline. Scale bars in **(F,F′)** apply to all six micrographs within the corresponding column. Abbreviations of SC layers as in **Figure 2**. Other abbreviations: CoIC, commissure of the IC; CoSC, commissure of the SC; PAG, periaqueductal gray matter.

ipsilateral TLC, which they enter at different rostrocaudal levels (**Figures 2C–F and 3C–F**). Upon entering the TLC by this route, SPON axons usually turn caudally and/or rostrally to span the nucleus longitudinally. Most of these axons seem to end within the ipsilateral TLC. However, some of them, particularly those traveling in the CoSC, give off collaterals for the ipsilateral TLC before crossing the midline to innervate the contralateral TLC or even proceeding into the contralateral SC (**Figures 2F and 3F**). The two routes taken by SPON axons that innervate the TLC are depicted schematically in **Figure 5**.

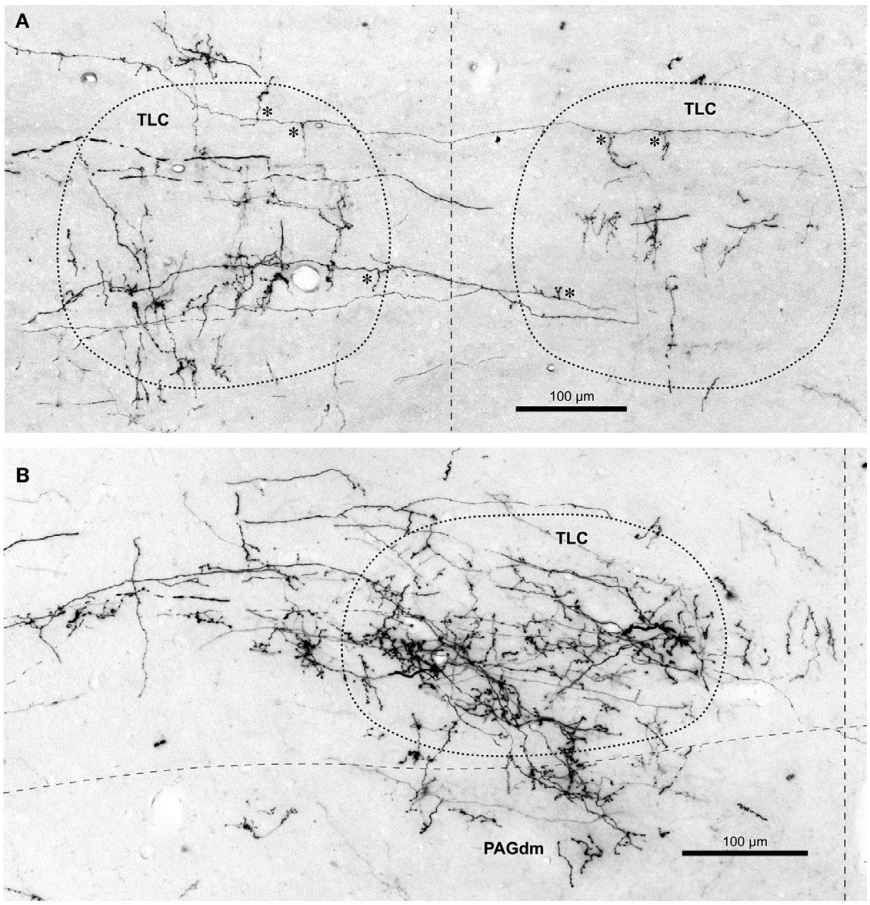

FIGURE 4 | Labeled terminal SPON fibers in the TLC. (A) Micrograph of a coronal section through the caudal portion of the left and right TLC after BDA was injected into the left SPON. Case 97097, whose injection site is depicted in **Figure 1B**. Several labeled SPON axons give off collateral branches (asterisks) within the ipsilateral and the contralateral TLC. Note the predominantly vertical orientation of the terminal axonal branches. **(B)** Micrograph of a coronal section through the central third of the TLC, Case 97084, whose injection site is depicted in **Figure 1B**. Numerous labeled fibers from the ipsilateral SPON enter the TLC from the SC and branch into thin collateral bearing abundant en passant and terminal boutons. Note terminal fibers entering the dorsomedial column of the PAG (PAGdm) from the overlying TLC. In both **(A,B)** the TLC has been delimited by dotted lines and the dashed vertical line indicates the midline.

It is evident from these observations that the projections from SPON to the ipsilateral and contralateral TLC are asymmetric. SPON fibers innervate densely the entire rostrocaudal length of the ipsilateral TLC, but only the caudal and rostral ends of the contralateral TLC (**Figures 2 and 3**).

The caudal third of the ipsilateral TLC is innervated preferentially by collaterals of axons that travel in the CoIC (**Figures 2A, B, 3A, B, 4A, and 5**), whereas the central and the rostral thirds of the nucleus are innervated mostly by axons that run through the deep layers of the SC (**Figures 2C–F, 3C–F, 4B, and 5**). The density of terminal SPON fibers is maximal in the central rostrocaudal third and decreases toward the caudal and the rostral ends of the TLC (**Figures 3 and 6**).

The caudal and the rostral portions of the contralateral TLC receive relatively sparse projections from the SPON by way of collaterals of axons that travel in the CoIC (**Figures 3A,B**) and the CoSC (**Figure 3F**), respectively. At every rostrocaudal level, the projection from SPON to the contralateral TLC is considerably less dense than the uncrossed projection (**Figure 6**).

The terminal branches of SPON axons within the TLC are variously oriented, although vertically oriented terminal fibers predominate at caudal levels on both sides (**Figures 3A′ and 4A**). Despite these varying orientations, the morphology of SPON axons is essentially similar on the two sides and remains rather constant at all rostrocaudal levels. Many terminal branches give off multiple short collaterals with one to three swellings, whereas others end in beaded branches bearing numerous small (<1.5 µm) *en passant* swellings and a terminal bouton (**Figure 4B**); all these varicosities and boutons are presumed to represent synaptic specializations.

TOPOGRAPHY OF PROJECTIONS FROM THE SPON TO THE TLC

Despite the fact that the projections from the SPON to the IC are clearly topographic and presumably tonotopic (Saldaña et al., 2009), no topographic organization is readily apparent in the projections from the SPON to the TLC. In all cases, regardless of the location of the injection site within SPON, labeled terminal fibers are widely distributed along the rostrocaudal

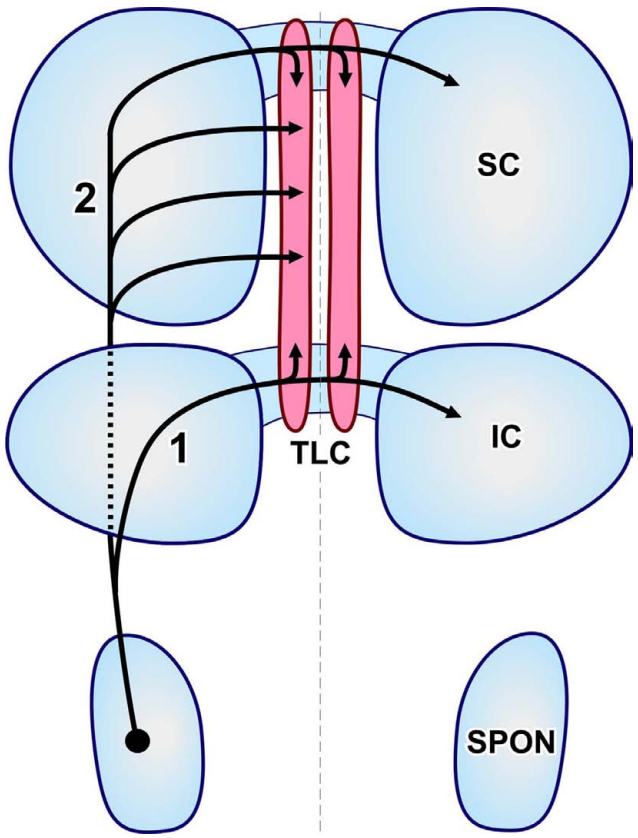

FIGURE 5 | Schematic representation of the routes followed by SPON axons that innervate the TLC. The projections have been superimposed on an idealized, dorsal view of the brainstem. The left and right TLC are shown in pink. The thin, vertical dashed line indicates the midline. Rostral is to the top. **(1)** Collaterals of axons that travel in the commissure of the IC. **(2)** Axons that reach the TLC by circumventing the IC (discontinuous line) and traveling through the deep layers of the SC.

and mediolateral axes of the TLC (**Figure 3**). The distribution of terminal fibers along the dorsoventral axis shows variations among different sections in a given case (for instance, in **Figures 3B,E** the labeled terminal fibers cover the entire dorsoventral diameter of the TLC, whereas in **Figures 3C,D** terminal fibers are concentrated in the ventral half of the nucleus; see also **Figure 6**).

Despite the above considerations, a subtle dorsoventral topography is appreciated at caudal levels. The terminal fields of SPON fibers tend to shift their dorsoventral position within the TLC as a function of the position of the injection site along the tonotopic (i.e., mediolateral) axis of the SPON (**Figures 7A1–A3,B1–B3**). Thus, in cases with tracer deposits in the medial (high characteristic frequency) region of the SPON, labeled terminal fibers are distributed mostly throughout the ventral half of the TLC; conversely, after injections in more lateral (lower characteristic frequency) regions of the SPON, labeled terminal fibers predominate dorsally within the TLC. This slight topographic tendency observed at caudal levels becomes gradually more difficult to discern rostrally (**Figures 7A4,A5,B4,B5**).

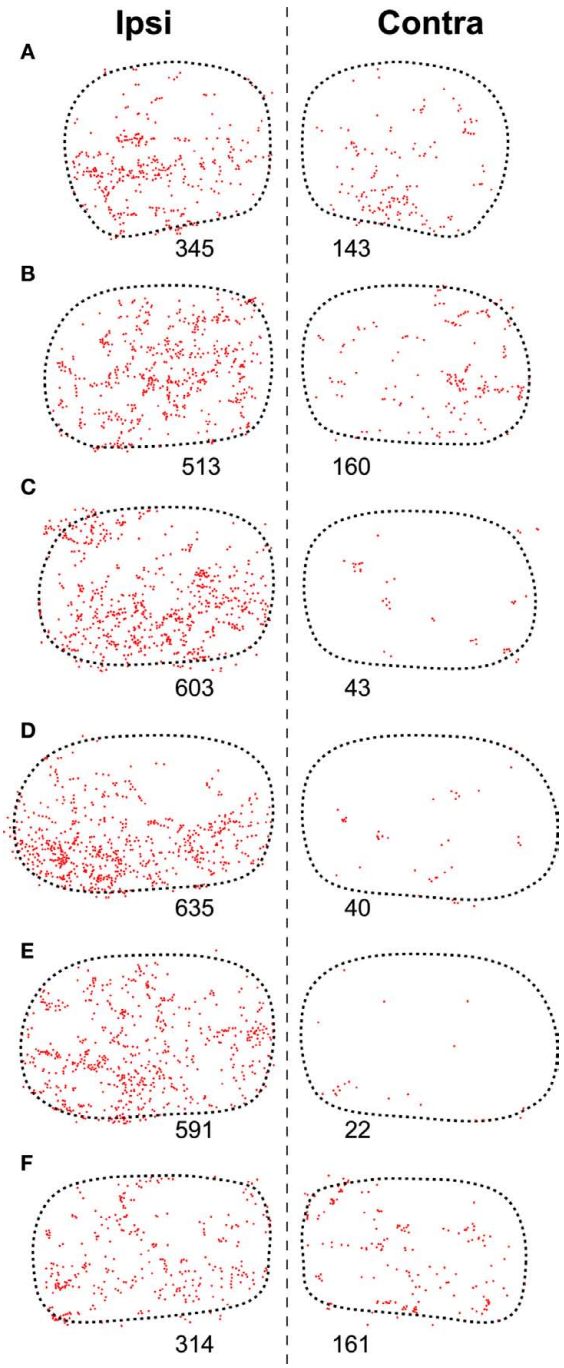

FIGURE 6 | Distribution of presumed synaptic boutons of SPON fibers in the TLC. (A–F) Plots of the location of all swellings and varicosities of SPON fibers labeled in the same sections of the TLC shown in **Figure 3** (Case 97084). Each dot represents one presumed bouton. The number below each TLC indicates the number of labeled boutons.

OTHER TARGETS OF SPON PROJECTIONS

Superior paraolivary nucleus neurons send projections to other targets besides the IC and the TLC. For example, even though many SPON axons that circumvent the IC appear to traverse the deep layers of the SC without branching, others give off collaterals that innervate the SC or the PAG (**Figures 2, 3, 4B, and 8**).

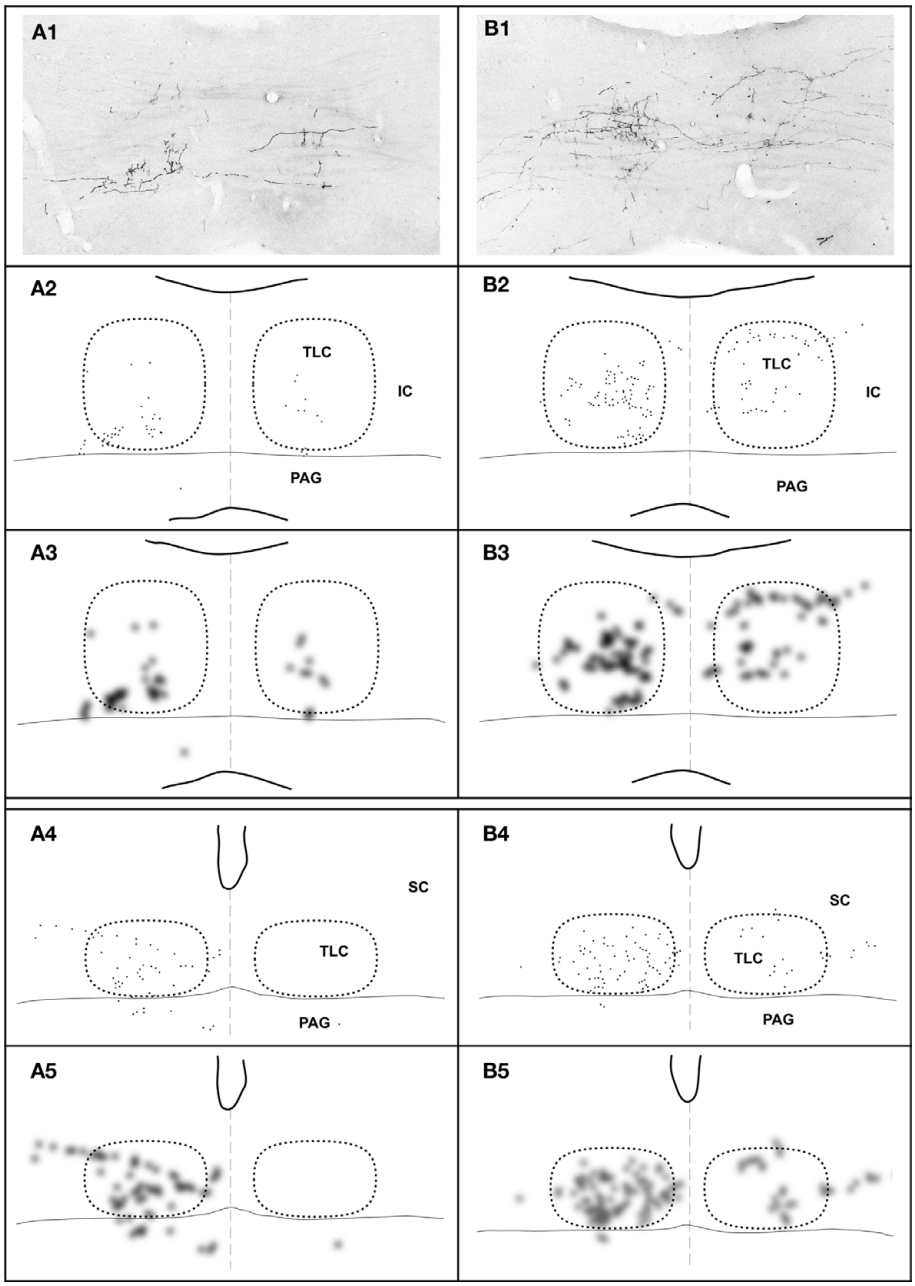

FIGURE 7 | Topography of the projection from the SPON to the TLC in two cases, whose injections of BDA were located in different positions along the mediolateral, tonotopic axis of the SPON. In case 97092 (left column) the injection site was located close to the medial border of the SPON (**Figure 1B**), whereas in case 97097 (right column) it was located in the lateral half of the SPON (**Figure 1B**). In each column, the image at the top **(A1,B1)** is a digital photomicrograph of a coronal section through the commissure of the IC (caudal third of the TLC). The second row **(A2,B2)** depicts a plot of the location of all labeled axonal swellings or varicosities (presumed to represent synaptic boutons) found in the microscopic field illustrated above. Each dot represents one axonal swelling or varicosity. The third row **(A3,B3)** shows a blurred image of the plots of the second row, in which the areas with the highest density of presumed synaptic boutons appear darkest. The fourth **(A4,B4)** and the fifth **(A5,B5)** rows show plots and blurred images of the distribution of the presumed synaptic boutons in a coronal section through the central rostrocaudal third of the TLC. In all panels, the right and the left TLC are delimited by dotted lines. Notice that the dorsoventral topography observed in caudal sections **(A3–B3)** becomes virtually lost at more rostral levels **(A5–B5)**.

In the SC ipsilateral to the injection site, labeled terminal fibers seem to concentrate in the caudal, ventral, and lateral region of the deep layers, not far from the rostral pole of the IC (**Figures 8A,B**). A few labeled collaterals ascend radially toward the intermediate and superficial layers, where terminal labeling is very sparse (**Figures 8A,C**). Very few labeled fibers are observed in layers of the ipsilateral SC more superficial than the intermediate gray layer (**Figures 2 and 8**).

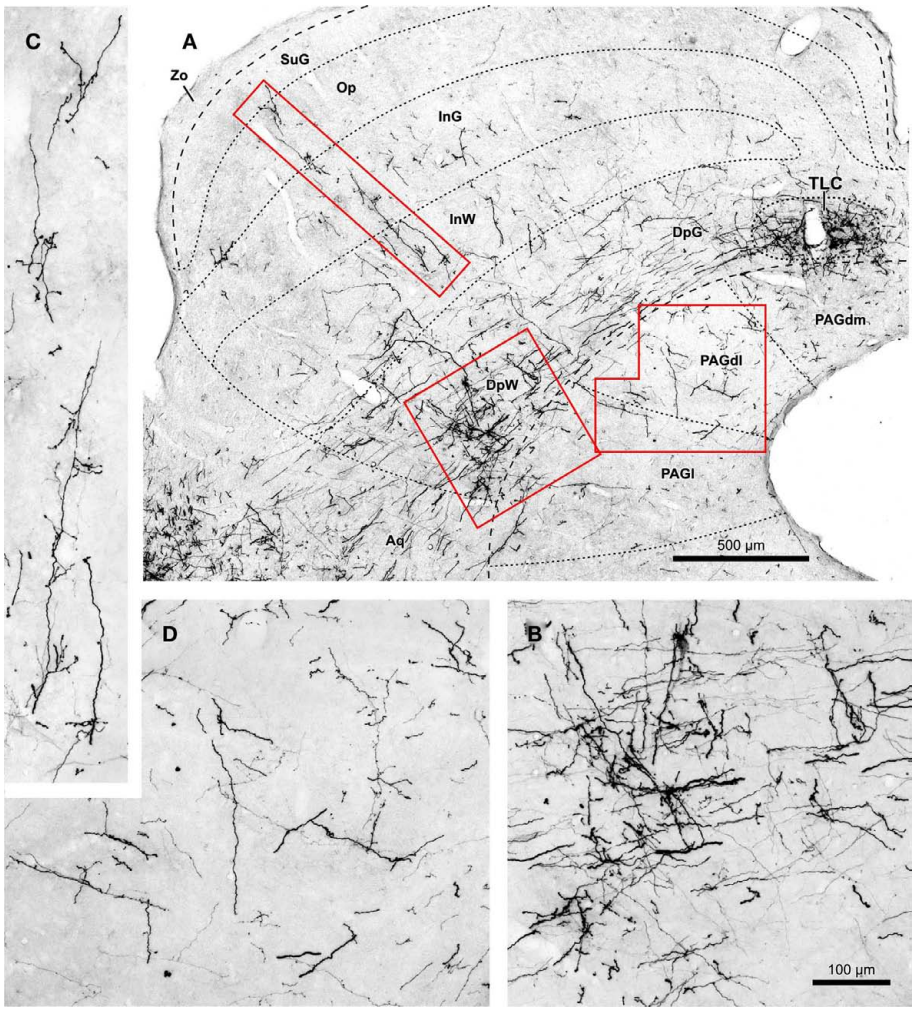

FIGURE 8 | (A) Micrograph of a coronal section of the midbrain tectum from a case that received an injection of BDA confined to the ipsilateral SPON. Case 97084, whose injection site is depicted in **Figure 1B**. The boxed areas are shown at higher magnification in **(B–D)**. **(B)** Terminal labeling in the ventrolateral part of the deep layers of the SC. **(C)** Labeled fibers that ascend radially toward the superficial layers of the SC. **(D)** Details of terminal fibers in the dorsolateral column of the PAG (PAGdl). Calibration bar in **(B)** applies also to **(C,D)**. Abbreviations of SC layers and PAG columns as in **Figure 2**.

Terminal labeling in the PAG ipsilateral to the injection site is sparse and widely distributed throughout the lateral, dorsolateral, and dorsomedial columns (**Figures 2, 3, and 8A,D**). In all cases, a few labeled fibers enter the dorsomedial column of the PAG from the overlying TLC (**Figure 4B**).

Terminal labeling is observed also in the SC and PAG contralateral to the injection site (**Figures 2 and 3**). These crossed projections are considerably less dense, however, than their ipsilateral counterparts.

Lastly, we also noted labeled terminal axons in the medial geniculate body ipsilateral to the injection site (**Figure 2F**). This novel projection from the SPON will be described in detail in a separate account.

RETROGRADELY LABELED NEURONS IN THE TLC

In most of our cases, retrogradely labeled cell bodies are found in the ipsilateral TLC (**Figure 9**), whereas neurons labeled in the contralateral TLC are very scarce (**Figure 9E**). The number of retrogradely labeled neurons varied from case to case and is apparently not related to the position of the injection site within the SPON. It is noteworthy that such retrogradely labeled neurons are always located within the territory occupied by SPON labeled terminal fibers (**Figure 9**), suggesting that the SPON and the TLC are reciprocally connected.

Most labeled TLC neurons display a punctate reaction product restricted to the cell body and, sometimes, the proximal dendritic segments; their axons are not labeled (**Figures 9A–E**). In the rare instances of neurons with diffuse labeling whose axons are labeled for hundreds of micrometers, no axonal collaterals are observed within the TLC (**Figure 9F**), suggesting that tectobulbar TLC neurons do not possess local recurrent collaterals.

Whereas close appositions between anterogradely labeled axonal swellings of SPON fibers and labeled cell bodies or dendrites in the TLC are occasionally observed, most axonal swellings are seen at a distance from retrogradely labeled neurons (**Figure 9**). This result suggests that SPON fibers preferentially target TLC neurons that do not innervate the SPON. However, we cannot rule out the

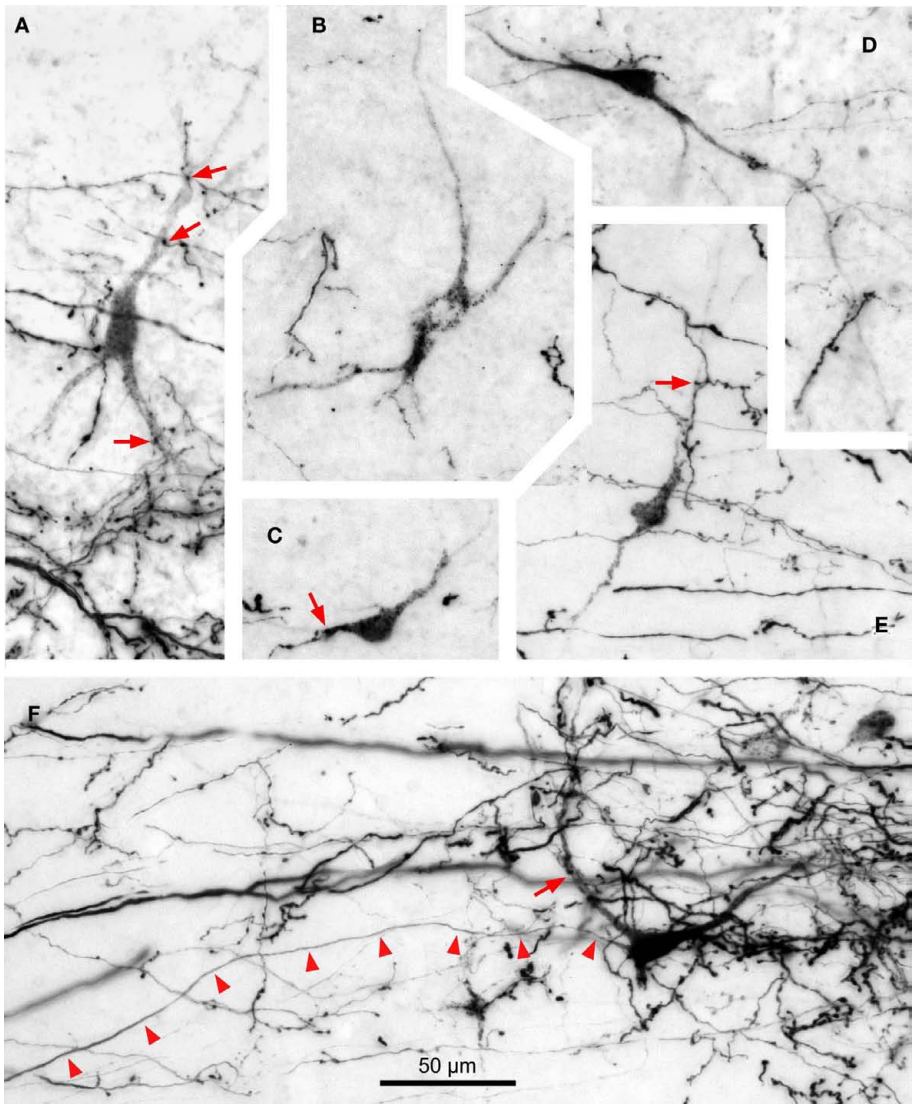

FIGURE 9 | Digital micrographs of TLC neurons retrogradely labeled following an injection of BDA into the SPON. Coronal sections. With the exception of **(E)**, all fields depict labeling in the TLC ipsilateral to the injection site. Note the multipolar morphology of the neurons, which are always intermingled with the terminal fiber fields formed by SPON axons. Red arrows indicate close appositions between boutons of labeled SPON axons and retrogradely labeled TLC neurons. Arrowheads in **(F)** point to the unbranched axon of a retrogradely labeled TLC neuron. **(A)** to **(D)** are from case 99044, and **(E,F)** from case 97084. Calibration bar in **(F)** applies to all micrographs.

possibility that SPON axons also innervate distal-most portions of the dendrites of tectobulbar TLC neurons that remained unlabeled in our experiments.

DISCUSSION

Our experiments have disclosed hitherto unknown projections from the SPON to the TLC of the rat, which constitute a major, novel auditory pathway through the lower brainstem to the midbrain. The SPON targets the entire ipsilateral TLC and, less densely, the caudal and rostral regions of the contralateral TLC. Our study also demonstrates that the SPON and the TLC are reciprocally connected, as the TLC contains abundant neurons that project back to the ipsilateral SPON.

TECHNICAL CONSIDERATIONS

In all our cases with injections of BDA into the SPON, numerous fibers were labeled in both the ipsilateral and contralateral TLC. This tracer is capable of giving rise to so-called collateral transport, whereby it labels anterogradely the collaterals of the axons through which it is transported retrogradely (i.e., Merchán et al., 1994; Warr et al., 1997; Doucet and Ryugo, 2003; Saldaña et al., 2009). Therefore, in principle, axons labeled with BDA may originate from neurons at the injection site (genuine anterograde transport) or may belong to neurons that innervate or cross the injection site (collateral transport). In our cases, numerous neurons were labeled in the ipsilateral medial nucleus of the trapezoid body (MNTB), and to a lesser extent in the contralateral ventral

cochlear nucleus and ipsilateral lateral nucleus of the trapezoid body (see also Saldaña et al., 2009). It is very unlikely, however, that the axons labeled in the TLC originated from these nuclei for two reasons: first, because labeled neurons are never found in any of these brainstem nuclei following deposits of the sensitive retrograde tracer FluoroGold into the paramedian region of the midbrain tectum that include large portions of the TLC within the injection site; and second, because labeled fibers are never found in the TLC following injections of BDA into the MNTB or the cochlear nuclei (unpublished observations).

In many of our cases, numerous neurons were retrogradely labeled within the TLC, but their axons were not visible (**Figure 9**). Moreover, the few retrogradely labeled neurons whose axons were labeled did not give off local collaterals (**Figure 9F**). Furthermore, labeled axons were systematically observed in the contralateral TLC, where retrogradely labeled neurons were extremely scarce. Finally, labeled axons in the TLC were observed in all cases with BDA injection into the SPON, including those that did not exhibit retrogradely labeled TLC neurons. Our interpretation, therefore, is that *all* BDA-labeled fibers in the TLC originate from the SPON.

THE SPON TO TLC PROJECTION

Our results demonstrate that the SPON sends direct projections to the TLC. These projections are predominantly ipsilateral, and seem to be dense. Given that the number of SPON neurons is relatively modest (approximately 2,500 neurons; Kulesza Jr. et al., 2002), the density of the projections revealed in this study indicates that the TLC is a main target of the SPON.

It has been known for decades that the main target of SPON projections is the ipsilateral IC (for references, see Saldaña et al., 2009). Given that virtually all SPON neurons participate in this projection (Saldaña and Berrebi, 2000), it is highly probable that SPON neurons that innervate the TLC also contribute to the innervation of the IC.

Recently, electrophysiological studies have demonstrated that, unlike neurons in the gerbil SPON, which exhibit considerable heterogeneity in their response properties (Behrend et al., 2002; Dehmel et al., 2002), neurons of the rat SPON are remarkably homogeneous. These cells are driven by input from the contralateral ear and strongly suppressed during acoustic stimulation by tonically active glycinergic inhibition that originates in the adjacent MNTB (Banks and Smith, 1992; Sommer et al., 1993; Smith et al., 1998; Kulesza Jr. et al., 2003; Kadner et al., 2006; Kadner and Berrebi, 2008). When the acoustic stimulus is terminated, SPON neurons are released from this inhibition and fire brief trains of discharges which constitute their characteristic offset response (Kulesza Jr. et al., 2003, 2007; Kadner and Berrebi, 2008). Because these offset spikes are triggered by episodes of low stimulus energy, i.e., gaps in ongoing stimuli and the troughs of amplitude modulated tones, Kadner and Berrebi (2008) proposed that the functional relevance of the brainstem MNTB/SPON circuit lies mainly in the encoding of *stimulus discontinuities*. The precisely timed output of the SPON is then relayed to its synaptic targets in the midbrain, including the TLC.

To understand the contribution of SPON projections to TLC function will require knowledge of the neuroactive substances released by SPON axons and the receptors expressed on the membranes of TLC neurons. Nothing is currently known regarding the latter issue, but several studies indicate that SPON neurons utilize GABA as their neurotransmitter (Mugnaini and Oertel, 1985; González-Hernández et al., 1996; Kulesza Jr. and Berrebi, 2000), so it is reasonable to assume that the projections described in this study are inhibitory. In the only detailed study to record the sound-evoked responses of TLC neurons, Marshall et al. (2008) reported no evidence for tonotopy in the nucleus, relatively broad frequency tuning and very limited sensitivity to amplitude modulation, even within the range of modulation frequencies that trigger highly synchronous action potentials from SPON neurons. Thus, it is difficult at this time to reconcile the physiological response properties of TLC neurons with the precisely timed offset spiking activity of SPON neurons. However, one must keep in mind that TLC neurons integrate their synaptic inputs from multiple sources, only a few of which are identified at this time, namely the auditory cortex (Morest and Oliver, 1984; Saldaña et al., 1996), the IC (Morest and Oliver, 1984; Saldaña and Merchán, 1992, 2005; Aparicio et al., 2010) and the SPON, as shown herein.

PROJECTION FROM THE TLC TO THE SPON

Based on the relatively high response thresholds and broad frequency tuning, as well as long first spike latencies, a prevalence for sustained firing patterns and poor phase-locking of TLC neurons, Marshall et al. (2008) concluded that the nucleus functions mainly in the descending modulation of lower auditory centers. This notion is supported by the fact that a large proportion of TLC neurons are immunolabeled by antisera directed against the inhibitory neurotransmitter GABA (our own unpublished immunohistochemical results) or its synthetic enzyme glutamic acid decarboxylase (Mugnaini and Oertel, 1985).

The present demonstration of TLC neurons retrogradely labeled from SPON injection sites confirms the existence of a descending projection and extends and refines previous studies that reported neurons labeled in the TLC following large deposits of retrograde tracers into the SOC (Faye-Lund, 1986; Mulders and Robertson, 2001; Saldaña et al., 2007). Thus, the SPON becomes the first identified target of TLC neurons.

It is also noteworthy that the TLC is the only documented source of descending inputs to the SPON of the rat, as this nucleus seems to be spared by other descending projections to the SOC (but see Thompson and Thompson, 1993; Coomes and Schofield, 2004, for results in the guinea pig). Indeed, descending IC fibers target preferentially the ventral nucleus of the trapezoid body (Faye-Lund, 1986; Caicedo and Herbert, 1993; Vetter et al., 1993; Mulders and Robertson, 2002). Likewise, the projections from the auditory cerebral cortex to the SOC terminate mainly in the ventral nucleus of the trapezoid body and, to a lesser extent, in the lateral superior olive and the so-called dorsal ribbon of the SOC (Feliciano et al., 1995; Mulders and Robertson, 2000).

CONCLUSION

The present tract-tracing investigation revealed two hitherto unknown connections in the rat auditory system: ascending projections from the SPON to the TLC and descending projections from the TLC to the SPON. Both the TLC and SPON have been identified in postmortem human brainstem (Saldaña et al., 2007; Kulesza Jr., 2008; Kulesza Jr. et al., 2011), leading us to believe that

the circuits discovered in the rat may also be present in humans. In any event, given our current level of understanding of the function of either nucleus, it is not possible at this time to formulate specific testable hypotheses of the biological significance of these reciprocal circuits. Electrophysiological recordings from the TLC while reversibly inactivating the SPON, or *vice versa*, would provide considerable insight into the impact of these reciprocal projections on auditory processing in the brainstem.

AUTHOR CONTRIBUTION

Enrique Saldaña designed the experiments and supervised the project. Antonio Viñuela and M.-Auxiliadora Aparicio performed the experiments and prepared the illustrations. Antonio Viñuela, M.-Auxiliadora Aparicio, Albert S. Berrebi, and Enrique Saldaña analyzed and interpreted the results. Enrique Saldaña and Albert S. Berrebi wrote the manuscript. Antonio Viñuela and M.-Auxiliadora Aparicio contributed equally to the work.

ACKNOWLEDGMENTS

This work was supported by the Spanish Ministries of Education and Science and Innovation grants PB95-1129, BFI2000/1358, BFU2004-05909, and BFU2008-04197 (to Enrique Saldaña), by the Junta de Castilla y León grants SA15/97, SA097/01, SA007C05, GR221, and Biomedicina 2009 (to Enrique Saldaña) and by the National Institute on Deafness and Other Communication Disorders Grant RO1 DC-002266 (to Albert S. Berrebi). The authors are thankful to Dr. Verónica Fuentes-Santamaría, who performed many of the tracing experiments.

REFERENCES

Aparicio, M. A., Viñuela, A., and Saldaña, E. (2010). Projections from the inferior colliculus to the tectal longitudinal column in the rat. *Neuroscience* 166, 653–664.

Bajo, V. M., Merchán, M. A., López, D. E., and Rouiller, E. M. (1993). Neuronal morphology and efferent projections of the dorsal nucleus of the lateral lemniscus in the rat. *J. Comp. Neurol.* 334, 241–262.

Banks, M. I., and Smith, P. H. (1992). Intracellular recordings from neurobiotin-labeled cells in brain slices of the rat medial nucleus of the trapezoid body. *J. Neurosci.* 12, 2819–2837.

Behrend, O., Brand, A., Kapfer, C., and Grothe, B. (2002). Auditory response properties in the superior paraolivary nucleus of the gerbil. *J. Neurophysiol.* 87, 2915–2928.

Caicedo, A., and Herbert, H. (1993). Topography of descending projections from the inferior colliculus to auditory brainstem nuclei in the rat. *J. Comp. Neurol.* 328, 377–392.

Coomes, D. L., and Schofield, B. R. (2004). Projections from the auditory cortex to the superior olivary complex in guinea pigs. *Eur. J. Neurosci.* 19, 2188–2200.

Dehmel, S., Doerrscheidt, G., and Reubsamen, R. (2002). Electrophysiological characterization of neurons in the superior paraolivary nucleus of the gerbil (*Meriones unguiculatus*). *Hear. Res.* 172, 18–36.

Doucet, J. R., and Ryugo, D. K. (2003). Axonal pathways to the lateral superior olive labeled with biotinylated dextran amine injections in the dorsal cochlear nucleus of rats. *J. Comp. Neurol.* 461, 452–465.

Faye-Lund, H. (1986). Projection from the inferior colliculus to the superior olivary complex in the albino rat. *Anat. Embryol.* 175, 35–52.

Feliciano, M., Saldaña, E., and Mugnaini, E. (1995). Direct projections from the rat primary auditory neocortex to nucleus sagulum, paralemniscal regions, superior olivary complex and cochlear nuclei. *Aud. Neurosci.* 1, 287–308.

González-Hernández, T., Mantolán-Sarmiento, B., González-González, B., and Pérez-González, H. (1996). Sources of GABAergic input to the inferior colliculus of the rat. *J. Comp. Neurol.* 372, 309–326.

González-Hernández, T. H., Meyer, G., Ferres-Torres, R., Castañeyra-Perdomo, A., and Pérez-Delgado, M. M. (1987). Afferent connections of the inferior colliculus in the albino mouse. *J. Hirnforsch.* 28, 315–323.

Henkel, C. K., and Shneiderman, A. (1988). Nucleus sagulum: projections of a lateral tegmental area to the inferior colliculus in the cat. *J. Comp. Neurol.* 271, 577–588.

Hutson, K. A., Glendenning, K. K., and Masterton, R. B. (1991). Acoustic chiasm. IV: eight midbrain decussations of the auditory system in the cat. *J. Comp. Neurol.* 312, 105–131.

Kadner, A., and Berrebi, A. S. (2008). Encoding of temporal features of auditory stimuli in the medial nucleus of the trapezoid body and superior paraolivary nucleus of the rat. *Neuroscience* 151, 868–687.

Kadner, A., Kulesza, R. J. Jr., and Berrebi, A. S. (2006). Neurons in the medial nucleus of the trapezoid body and superior paraolivary nucleus of the rat may play a role in sound duration coding. *J. Neurophysiol.* 95, 1499–1508.

Kulesza, R. J. Jr. (2008). Cytoarchitecture of the human superior olivary complex: nuclei of the trapezoid body and posterior tier. *Hear. Res.* 241, 52–63.

Kulesza, R. J. Jr., and Berrebi, A. S. (2000). The superior paraolivary nucleus of the rat is a GABAergic nucleus. *J. Assoc. Res. Otolaryngol.* 1, 255–269.

Kulesza, R. J. Jr., Kadner, A., and Berrebi, A. S. (2007). Distinct roles for glycine and GABA in shaping the response properties of neurons in the superior paraolivary nucleus of the rat. *J. Neurophysiol.* 97, 1610–1620.

Kulesza, R. J. Jr., Lukose, R., and Stevens, L. V. (2011). Malformation of the human superior olive in autistic spectrum disorders. *Brain Res.* 1367, 360–371.

Kulesza, R. J. Jr., Spirou, G. A., and Berrebi, A. S. (2003). Physiological response properties of neurons in the superior paraolivary nucleus of the rat. *J. Neurophysiol.* 89, 2299–2312.

Kulesza, R. J. Jr., Viñuela, A., Saldaña, E., and Berrebi, A. S. (2002). Unbiased stereological estimates of neuron number in subcortical auditory nuclei of the rat. *Hear. Res.* 168, 12–24.

Marshall, A. F., Pearson, J. M., Falk, S. E., Skaggs, J. D., Crocker, W. D., Saldaña, E., and Fitzpatrick, D. C. (2008). Auditory response properties of neurons in the tectal longitudinal column of the rat. *Hear. Res.* 244, 35–44.

Merchán, M. A., Saldaña, E., and Plaza, I. (1994). Dorsal nucleus of the lateral lemniscus in the rat: concentric organization and tonotopic projection to the inferior colliculus. *J. Comp. Neurol.* 342, 259–278.

Morest, D. K., and Oliver, D. L. (1984). The neuronal architecture of the inferior colliculus in the cat: defining the functional anatomy of the auditory midbrain. *J. Comp. Neurol.* 222, 209–236.

Mugnaini, E., and Oertel, W. H. (1985). "An atlas of the distribution of GABAergic neurons and terminals in the rat CNS as revealed by GAD immunohistochemistry," in *Handbook of Chemical Neuroanatomy*, Vol. 4, *GABA and Neuropeptides in the CNS*, Part I, eds A. Bjorklund and T. Hokfelt (Amsterdam: Elsevier Science Publishers), 436–608.

Mulders, W. H., and Robertson, D. (2000). Evidence for direct cortical innervation of medial olivocochlear neurones in rats. *Hear. Res.* 144, 65–72.

Mulders, W. H., and Robertson, D. (2001). Origin of the noradrenergic innervation of the superior olivary complex in the rat. *J. Chem. Neuroanat.* 21, 313–322.

Mulders, W. H., and Robertson, D. (2002). Inputs from the cochlea and the inferior colliculus converge on olivocochlear neurones. *Hear. Res.* 167, 206–213.

Paxinos, G., and Watson, C. (2007). *The Rat Brain in Stereotaxic Coordinates*, 6th Edn. San Diego: Academic Press.

Saldaña, E., Aparicio, M. A., Fuentes-Santamaría, V., and Berrebi, A. S. (2009). Connections of the superior paraolivary nucleus of the rat: projections to the inferior colliculus. *Neuroscience* 163, 372–387.

Saldaña, E., and Berrebi, A. S. (2000). Anisotropic organization of the rat superior paraolivary nucleus. *Anat. Embryol.* 202, 265–279.

Saldaña, E., Feliciano, M., and Mugnaini, E. (1996). Distribution of descending projections from primary auditory neocortex to inferior colliculus mimics the topography of intracollicular projections. *J. Comp. Neurol.* 371, 15–40.

Saldaña, E., and Merchán, M. A. (1992). Intrinsic and commissural connections of the rat inferior colliculus. *J. Comp. Neurol.* 319, 417–437.

Saldaña, E., and Merchán, M. A. (2005). "Intrinsic and commissural connections of the inferior colliculus," in *The Inferior Colliculus*, eds J. A. Winer and C. E. Schreiner (New York: Springer), 155–181.

Saldaña, E., Viñuela, A., Marshall, A. F., Fitzpatrick, D. C., and Aparicio, M. A. (2007). The TLC: a novel auditory nucleus of the mammalian brain. *J. Neurosci.* 27, 13108–13116.

Smith, P. H., Joris, P. X., and Yin, T. C. (1998). Anatomy and physiology of principal cells of the medial nucleus of the trapezoid body (MNTB) of the cat. *J. Neurophysiol.* 79, 3127–3142.

Sommer, I., Lingenhohl, K., and Friauf, E. (1993). Principal cells of the rat

medial nucleus of the trapezoid body: an intracellular in vivo study of their physiology and morphology. *Exp. Brain Res.* 95, 223–239.

Thompson, A. M., and Thompson, G. C. (1993). Relationship of descending inferior colliculus projections to olivocochlear neurons. *J. Comp. Neurol.* 335, 402–312.

Vetter, D. E., Saldaña, E., and Mugnaini, E. (1993). Input form the inferior colliculus to medial olivocochlear neurons in the rat: a double label study with PHA-L and cholera toxin. *Hear. Res.* 70, 173–186.

Warr, W. B., Boche, J. B., and Neely, S. T. (1997). Efferent innervation of the inner hair cell region: origins and terminations of two lateral olivocochlear systems. *Hear. Res.* 108, 89–111.

Conflict of Interest Statement: The authors declare that the research was conducted in the absence of any commercial or financial relationships that could be construed as a potential conflict of interest.

Received: 23 July 2010; paper pending published: 06 September 2010; accepted: 05 January 2011; published online: 22 February 2011.

Citation: Viñuela A, Aparicio M-A, Berrebi AS and Saldaña E (2011) Connections of the superior paraolivary nucleus of the rat: II. Reciprocal connections with the tectal longitudinal column. Front. Neuroanat. ***5****:1. doi: 10.3389/fnana.2011.00001*